The Quasicrytalline Spin-Network — a Chiral Icosahedral Quasicrystal derived from $\mathbf{E_8}$

F. Fang* and K. Irwin

Quantum Gravity Research, Los Angeles, CA, U.S.A.

We present the construction of an icosahedral quasicrystal, a quasicrystalline spin network, obtained by spacing the parallel planes in an icosagrid according to the Fibonacci sequence. This quasicrystal can be thought of as a golden composition of five sets of Fibonacci tetragrids. This quasicrystal embeds the quasicrystals that are *golden* compositions of the three-dimensional tetrahedral cross-sections of the Elser-Sloane quasicrystal, which is a four-dimensional cut-and-project set of the E_8 lattice. These compound quasicrystals are subsets of the quasicrystalline spin network, and the former can be enriched to form the later. This creates a mapping between the quasicrystalline spin network and the $\mathbf{E_8}$ lattice.

I. Introduction

Until Shechtman et al.[22] discovered a quasicrystal in nature, crystallographic rules prohibited their existence. This discovery intrigued scientists from various disciplines, such as math, physics, materials science, chemistry and biology[1,14,19,21,25]. In the early years, there was a surge in the interest in studying the mathematical aspects of quasicrystals[4,10,12,15,17,23,24]. In recent years, the majority of research in the field has shifted toward the physical aspects of quasicrystals, such as their electronic and optical properties[7,18] and growth[9]. The mathematical properties of quasicrystals are still relatively unexplored. Investigation in this field provides opportunity for discoveries that could have far reaching consequences in physics and other disciplines.

In this paper, we introduce an icosahedral quasicrystal, the quasicrystalline spin network (QSN). It is a superset of a golden ratio based composition of three-dimensional slices of the four-dimensional Elser-Sloane quasicrystal projected from E_8[6,16]. We focus on the geometric connections between the quasicrystalline spin-network and the E_8 lattice.

This paper includes six sections. In section II, we briefly introduce the definition of a quasicrystal and the usual methods for generating them mathematically. Then using Penrose tilling as an example, we introduce a new method - the Fibonacci multigrid method - in addition to the cut-and-project[3] and dual-grid methods[24]. In section III, we applie the Fibonacci multigrid method in three dimensions and obtain an icosahedral quasicrystal, the Fibonacci icosagrid which we call the quasicrystalline spin network. We also explain an alternative way of generating it using five sets of tetragrids. This new way of constructing this quasicrystal revealed a direct connection between this quasicrystal and a compound quasicrystal that is introduced in Section IV. Important properties of the Fibonacci icosagrid are discussed. For example, its vertex configurations, edge-crossing types and space-filling analog. Section IV introduces the compound quasicrystal that is obtained from a projection/slicing/composition of the E_8 lattice. It starts with a brief review of the Elser-Sloane quasicrystal and then introduces two three-dimensional compound quasicrystals that are composites of three-dimensional tetrahedral slices of the Elser-Sloane quasicrystal. We also introduce an icosahedral slice of the Elser-Sloane quasicrystal that is itself a quasicrystal with the same unit cells as the space-filling analog of the QSN. Section V compares the Fibonacci icosagrid to the compound quasicrystals obtained from the Elser-Sloane quasicrystal and demonstrates the connection between them, suggesting a possible mapping between QSN and the E_8 lattice. The last section, Section VI summarizes the paper.

II. Fibonacci Multigrid Method

While there is still no commonly agreed upon definition of a quasicrystal[12,13,21], it is generally believed that for a structure to be a quasicrystal, it should have the following properties:

1. It is ordered but not periodic.
2. It has long-range quasiperiodic translational order and long-range orientational order. In other words, for any finite patch within the quasicrystal, you can find an infinite number of identical patches at other locations, with translational and rotational transformation.
3. It has finite types of prototiles/unit cells.
4. It has a discrete diffraction pattern.

Mathematically, there are two common ways of generating a quasicrystal: a cut-and-project from a higher

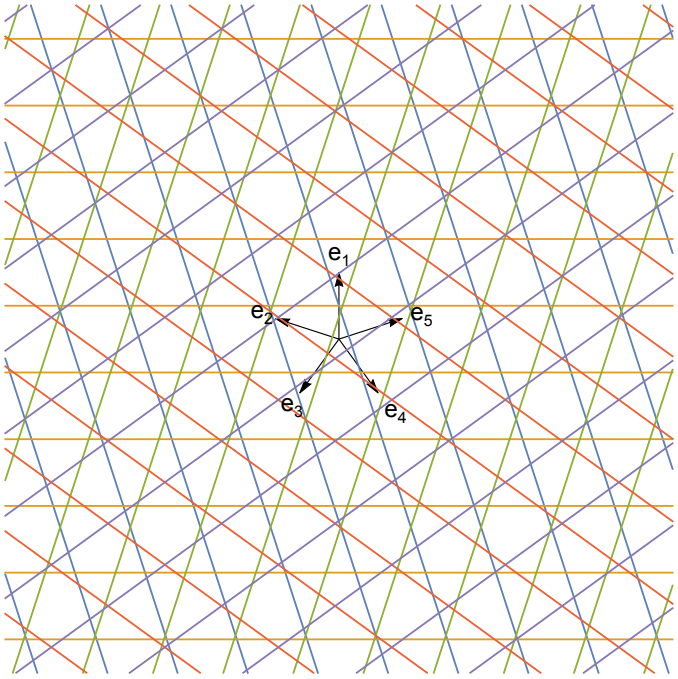

Figure 1: *An example of a pentagrid, with e_1, e_2,...,e_5 being the norm of the grids.*

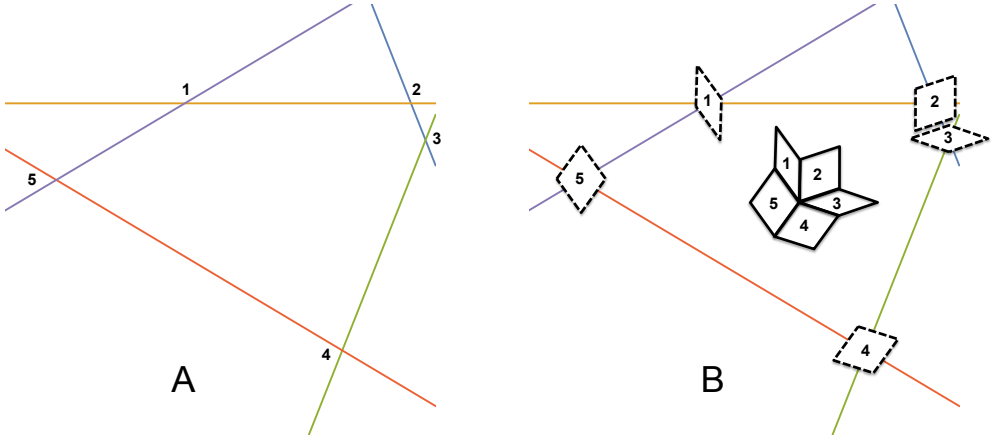

Figure 2: *A) Identify the intersections in a sample patch in pentagrid, B) construct a dual quasicrystal cell, here the prolate and oblate rhombs, at each intersect point and then place them edge-to-edge while maintaining their topological connectedness.*

dimensional crystal[21,24] and the dual grid method[21,24]. We independently developed a new method, the Fibonacci multigrid method, for generating a quasicrystal. This method is a special case of the generalized dual grid method discussed in Socolar, et al[24], which focuses on the cell space instead of the grid space, on which we are focused. We introduce this method in the next few paragraphs, using the the pentagrid and its dual quasicrystal, Penrose tiling, as an example.

The commonly used dual grid for generating a Penrose tiling is called the pentagrid and it is a periodic grid. Fig. 1 gives an example of a pentagrid. A pentagrid is defined as (Fig. 1)

$$\vec{x} \cdot \vec{e} = x_N, N \in Z, , \tag{1}$$

with

$$e_n = \left(\cos\frac{2\pi n}{5}, \sin\frac{2\pi n}{5}\right), n = 0, 1, ..., 4 \tag{2}$$

$$x_N = T(N + \gamma), \tag{3}$$

where $e_n, n = 0, 1, ...4$, are the norms of the parallel grid lines, T is constant and it specifies the equal spacing between the parallel grid lines. In other words, the period of x_N, γ is a real number and it corresponds to the phase or offset of the grid with respect to the origin. Fig. 2 shows the process of constructing a Penrose tiling with this pentagrid:

1. First we identify all the intersections in the pentagrid ($1-5$ in Fig. 2A). There are only two types of intersections in the grid (in Fig. 2A, 1 and 3 are

Corresponding Author •fang@quantumgravityresearch.org

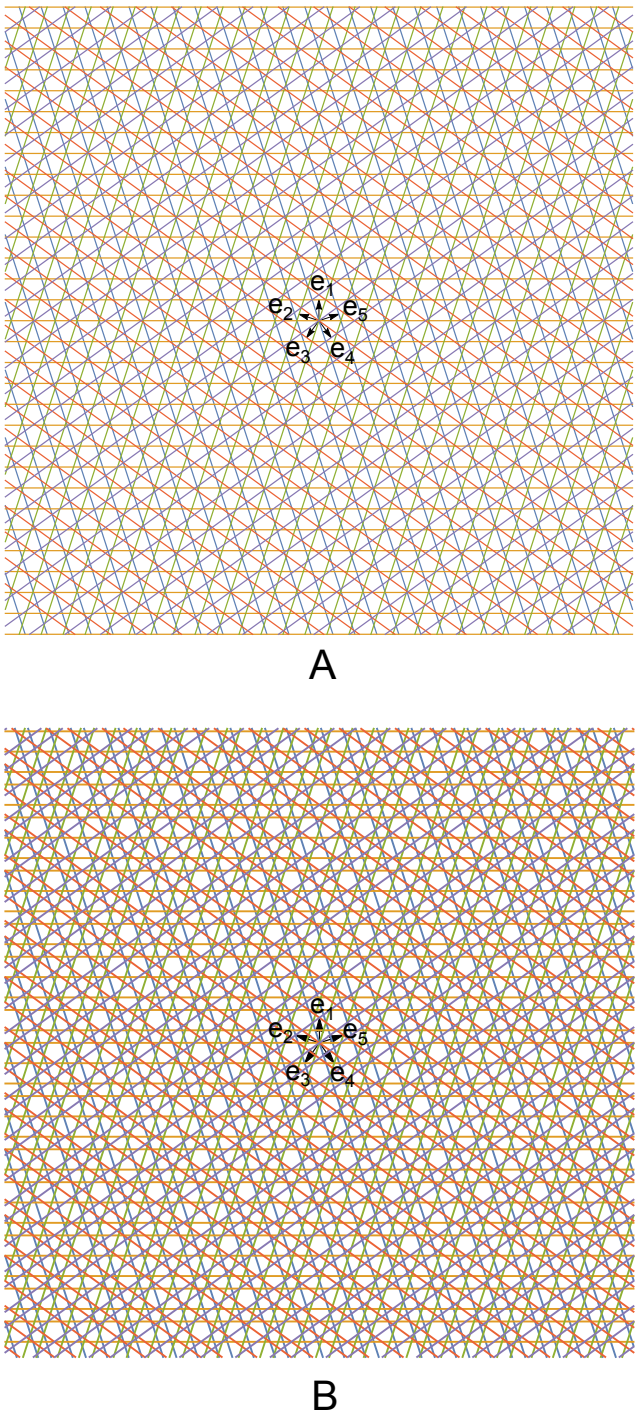

Figure 3: *A) Pentagrid and B) Fibonacci pentagrid - quasicrystalized pentagrid using Fibonacci-sequence spacing.*

the same and 2, 4 and 5 are the same), specified by the angle of intersection.

2. At each intersection point, a dual quasicrystal cell can be constructed (Fig. 2B). The edges of the cell are perpendicular to the grid lines that the edges cross. Thus two types of intersections result in two types of quasicrystal cells, the prolate and oblate rhombi shown in Fig. 2B.

3. The last step is to place the rhombi edge-to-edge while maintaining their original topological connectedness. For example, as shown in Fig. 2B, although the cells are translated to be placed edge-to-edge, cell 1 is always connected to cell 2 through the vertical edge, cell 2 is connected to cell 3 through the other non-vertical edge, and so on.

If the values of the offset γ are properly chosen so that there are no more than two lines intersecting at one point (to avoid glue tiles[24]), the resulting quasicrystal will be a Penrose tiling. As we can see from this procedure, eventually, each vertex (intersection) in the pentagrid will correspond to a cell in the Penrose tiling, and each

vertex in the Penrose tiling will correspond to a cell in the pentagrid. Therefore the grid space and the cell space are dual to each other.

Although its dual is a quasicrystal, the pentagrid itself is not a quasicrystal due to the arbitrary closeness (infinite number of unit cells) between the vertices(Fig. 3A). We independently discovered a modification that can be applied to the periodic grid to make the grid itself quasiperiodic. This method has already introduced by Socolar et. al. in 1986. The modification is to change the Eq. 3 from periodic to quasiperiodic[24]):

$$x_N = T(N + \alpha + \frac{1}{\rho}\left\lfloor \frac{N}{\mu} + \beta \right\rfloor), \tag{4}$$

where α, β, and $\rho \in R$, μ are irrational, and $\lfloor\rfloor$ is the floor function and denotes the greatest integer less than or equal to the argument. Since N can be all integers, including negative ones, we can set all the other variables in this expression to be positive without losing its generality. This expression defines a quasiperiodic sequence of two different spacings, L and S, with a ratio of $1 + 1/\mu$. Changing μ, α and β can change the relative frequency of the two spacings, the offsets of the grid and the order of the sequence of the two spacings, respectively.

This paper focuses on a special case of the quasiperiodic grid, where $\rho = \mu = \tau$ and $\tau = \frac{1+\sqrt{5}}{2}$ is the golden ratio. In this case, x_N defines a Fibonacci sequence[12]. The modified pentagrid is called Fibonacci Pentagrid. Not only is its dual a quasicrystal(a Penrose tiling), but it can be shown that the Fibonacci pentagrid itself is also a quasicrystal. You can clearly see in Fig. 3B that there are finite types of unite cells in the Fibonacci pentagrid and the arbitrary closeness disappeared.

We call this method the Fibonacci multigrid. Using this method, we generate a three-dimensional icosahedral quasicrystal discussed in the following sections.

III. Fibonacci IcosaGrid

3.1 Icosagrid and tetragrid

An icosagrid is a three-dimensional planar periodic 10-grid where the norm vectors of the ten planar grid, $e_n, n = 1, 2, ...10$, coincide with the ten threefold symmetry axis of an icosahedron as shown in Fig. 4. With this specification of these norm vectors, an icosagrid can be generated using Eq. 1-3 with $\gamma = 0$. This icosagrid dissects the three-dimensional space into infinite types of three-dimensional cells. However, we present properties of the icosagrid when only the regular tetrahedral cells (Fig. 5) are "turned on". The first of these properties is that this structure can be separated into two chiral structures with opposite handedness. Fig. 6 shows how these two structures with opposite chiralities can be separated from the icosagrid. The second property is that the icosagrid can be built in an alternative way using five sets of tetragrids. The details are discussed in the following paragraphs.

Similar to an icosagrid, a tetragrid is defined as a three-dimensional planar periodic 4-grid where the norm vectors of the four planar grid, $e_n, n = 1, 2, ...4$, coincide with the four threefold symmetry axis of a tetrahedron. When $\gamma = 0$, the tetragrid becomes a periodic FCC lattice which can be thought of as a space-filling combination of regular tetrahedral cells of two orientations and octahedral cells (Fig. 7). Tetrahedra of the two orientations share the same point set (tetrahedral vertex). The icosagrid can be thought of as a combination of five sets of tetragrids, composed together with a golden composition procedure achieved in the following manner(Fig. 8):

1. We start from the origin in the tetragrid and identify the eight tetrahedral cells sharing this point with four being in one orientation and the other four in the dual orientation (yellow tetrahedra in Fig. 8A).

2. We pick the four tetrahedral cells of the same orientation (Fig. 8B) and make four copies.

3. We place two copies together so that they share their center point and the adjacent tetrahedral faces are parallel, touching each other and with a relative rotation angle of $Cos^{-1}(\frac{3\tau-1}{4})$, the golden rotation[8] (Fig. 8C).

4. We repeat the process three more times to add the other three copies to this structure (Fig. 8C, D, E). A twisted 20-tetrahedra cluster, the 20-group (20G)(Fig. 8F), is formed.

5. We now expand the tetragrid associated with each of the 4-tetrahedra sets by turning on the tetrahedra of the same orientation as the existing four. An icosagrid of one chirality is achieved(Fig. 6A). Similarly, if the tetrahedral cell of the other orientation are turned on, an icosagrid of the opposite chirality will be achieved (Fig. 6C).

In either case of the handedness, there is a 20G at the center of the structure. Fig. 9A and C show the two chiralities (or handedness). We call one left-twisted and other other right-twisted of the 20G respectively and Fig. 9 A shows the superposition of both chiralities. The two chiralities share the same point set (the 61 tetrahedral vertices in the 20G, the pink points shown in Fig. 9) but have different connections turned on (blue or red as shown in Fig. 9). The fact that tuning on these tetrahedral cells split the icosagrid into two chiralities is interesting and provoked the further investigation into this structure. From this point on, we refer to the icosagrid as this set of tetrahedral cells (or tetrahedra). In terms of tetrahedral packing, the center 20G is a dense packing of 20 tetrahedra with maximally reduced plane class (parallel plane set). It groups the 20 tetrahedra into a minimum of five crystal groups (the maximum number of vertex sharing tetrahedral clusters in a crystalline arrangement that is divisible by 20 is 4). Therefore the plane classes are reduced to a minimum number of 10, compared with the 70 plane classes in the evenly distributed vertex-sharing 20-tetrahedra cluster shown in Fig. 10. One can also see that from the evenly distributed vertex-sharing-20-tetrahedra cluster to the 20G, the golden twisting "shifts" the gaps between the tetrahedral faces to the canonical pentagonal cones, one of which is marked with a white circled arrow in Fig. 10B. In other words, these canonical pentagonal cones

Corresponding Author •fang@quantumgravityresearch.org

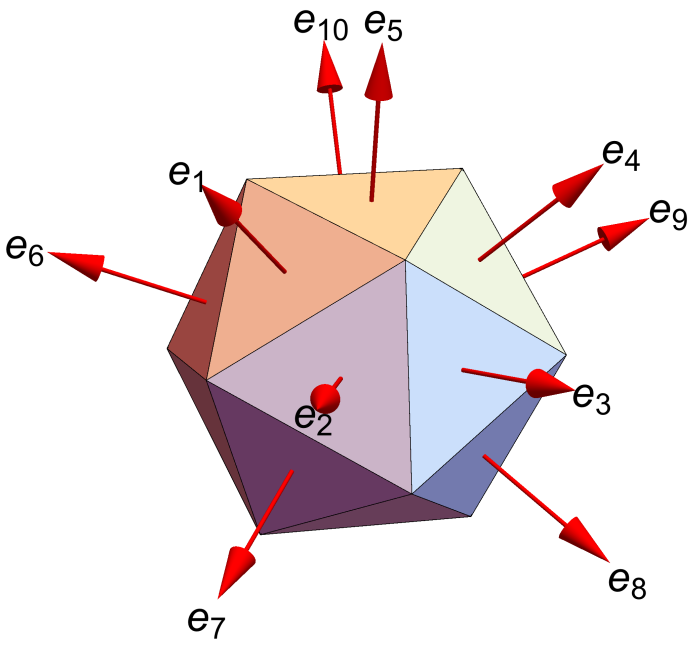

Figure 4: *The norm vectors of the icosagrid:* e_1, e_2,...,e_{10}.

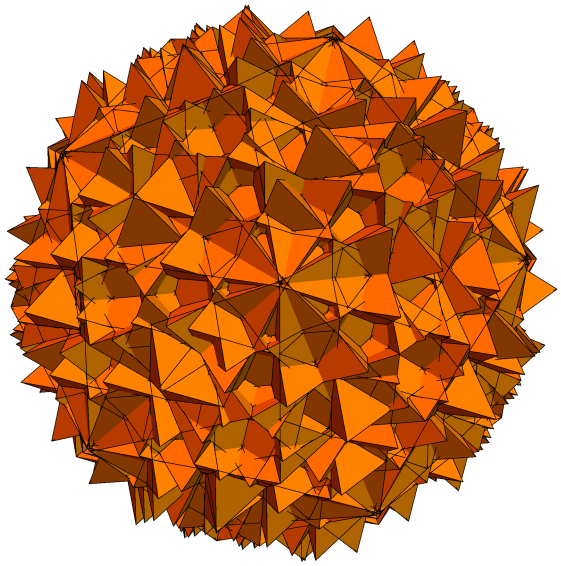

Figure 5: *Icosagrid with regular tetrahedral cells shown.*

are a signature of the maximum plane class reduction in the vertex-sharing 20-tetrahedra packing.

The Fibonacci icosagrid

The icosagrid, like the pentagrid, is not a quasicrystal due to the arbitrary closeness and therefore the infinite number of cell shapes it posesses. Also it does not satisfy the second property of a quasicrystal mentioned in section II: for any finite patch in the quasicrystal, one can find an infinite number of identical patches at other locations, under translation and/or rotation. For example, there is no other 20G possible in an icosagrid of infinite size. In order to convert the icosagrid to a quasicrystal, just as how we converted the pentagrid to the Fibonacci pentagrid, we use Eq. 4 instead of Eq. 3 for x_N. As a result, the spacings between the parallel planes in the icosagrid becomes the Fibonacci

Corresponding Author •fang@quantumgravityresearch.org

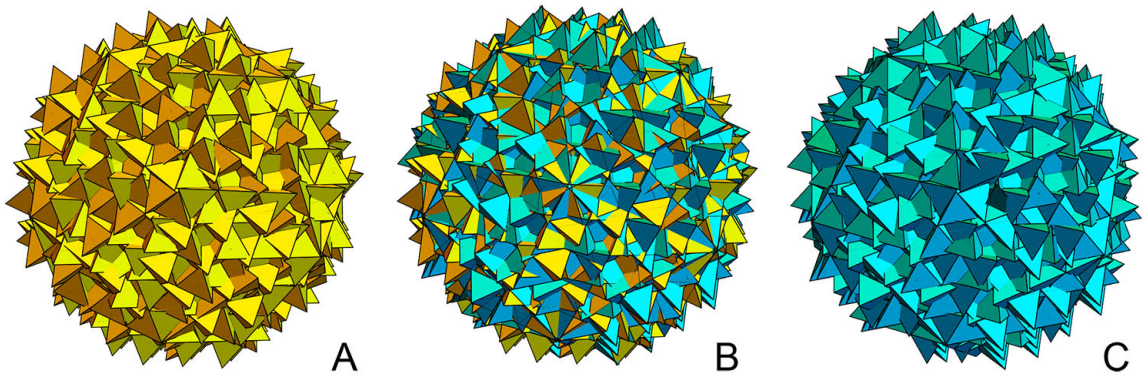

Figure 6: *Icosagrid (B) separated into two opposite chiralities: left A) and right C).*

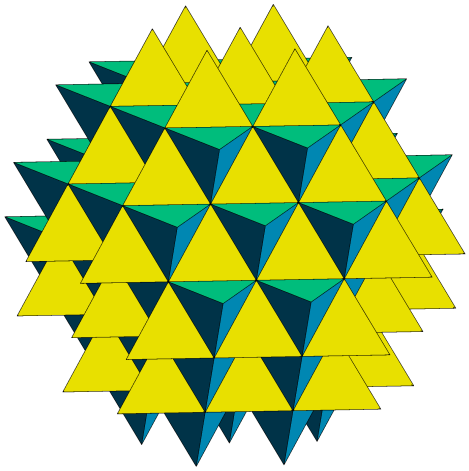

Figure 7: *Tetragrid with tetrahedral cells of two different orientation (Yellow and Cyan) and Octahedral gaps.*

sequence. A 2D projection of one of the tetragrids before and after this modification is shown in Fig. 11A and Fig. 11B respectively. Each tetragrid becomes a Fibonacci tetragrid and the icosagrid becomes the Fibonacci icosagrid (Fig. 11C).

In the Fibonacci icosagrid, 20Gs appear at the various locations beside the center of the structure (marked with white dotted circles in Fig. 11C). The arbitrary closeness is removed and there are finite types of local clusters. We investigated the local clusters with the nearest neighbor configuration around a vertex (the vertex configuration)[26] and the detailed results will be published soon. We will briefly discuss the results in this paper. We introduce a term, degree of connection, to the vertex configurations. It is defined as the number of unit length connections a vertex has. The minimum degree of connection for the vertices in the Fibonacci icosagrid is three and the maximum degree of connection is 60. Also, since the Fibonacci icosagrid is a collection of five-tetrahedra sets (the tetrahedra are of the same orientation in each set), there are only 30 unit-length edge classes (tetrahedra of each orientation have six edge classes). From the above facts, it is not hard to deduce that there is a finite amount of vertex configurations in the Fibonacci icosagrid. A sample of the vertex configurations is shown in Fig. 12. Our following paper will also discuss how all the vertices of the Fibonacci icosagrid live in the Dirichlet integer space–integers of the form $a + b\tau$ where a and b are integers. We have noticed that the edge-crossing points (edge intersection points) in the Fibonacci icosagrid also live in the Dirichlet integer space. We define the edge-crossing configurations as with p/q where p is the ratio of the segments the edge-crossing point divide the first edge into and q is the ratio for the second edge. There is a finite amount of types of the edge-crossing configurations and the value for p and q are simple expressions with the golden ratio. The diffraction pattern of the 5-fold axis is shown in Fig. 13. The 2-fold and 3-fold diffraction patterns are also seen from the Fibonacci icosagrid. This indicates that the Fibonacci icosagrid is a three-dimensional quasicrystal with icosahedral symmetry, considering only the point set and/or the connections of both chiralities. The symmetry reduces to a chiral icosahedral symmetry if we consider the connections of only one handedness.

The quasicrystal in the cell space of the Fibonacci icosagrid is similar to the three-dimensinal Ammann-Beenker tiling[12] which will not be discussed in this paper. We have investigated another way to generate a space-filling analog of the Fibonacci icosagrid that is isomorphic to a subspace of the quasicrystal in the cell space of the Fibonacci icosagrid. Most of the vertices of this quasicrystal are the centers of the regular tetrahedral cells in the Fibonacci icosagrid. There are three types of intersecting polyhedral cells: the icosahedron, dodecahedron and the icosidodecahedron. Fig. 14A shows the point set of this quasicrystal and some of the polyhedral cells. This kind of quasicrystal is very common in nature[11,27].

IV. The Quasicrystals derived from E_8

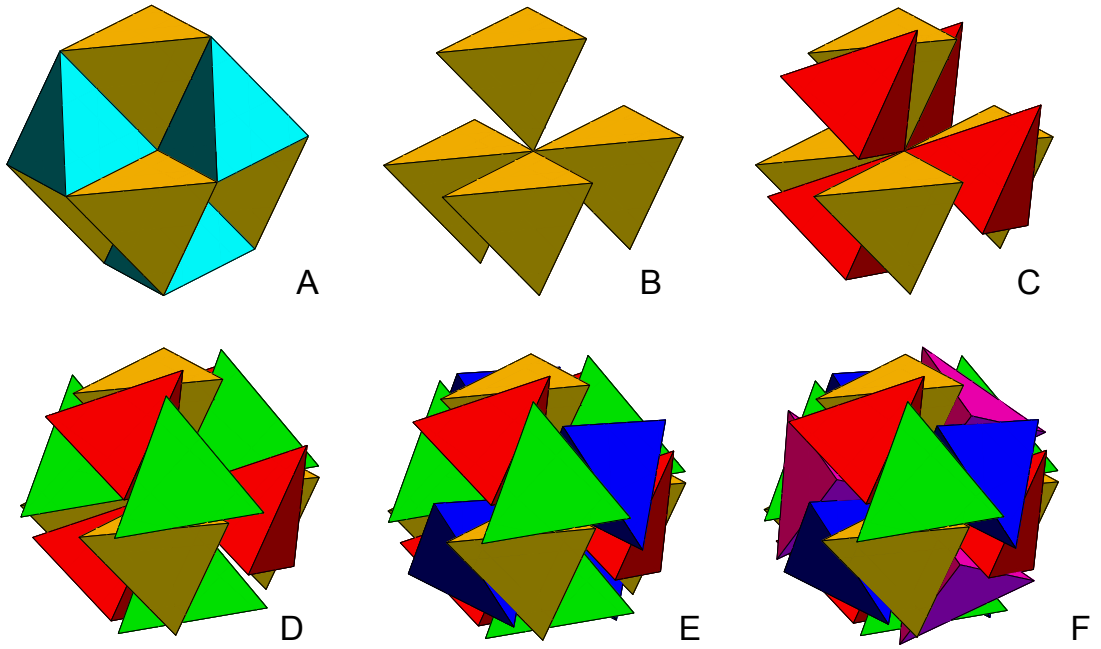

Figure 8: *(A) A small tetragrid local cluster with eight tetrahedral cells, four "up" and four "down". B-F) The golden composition process).*

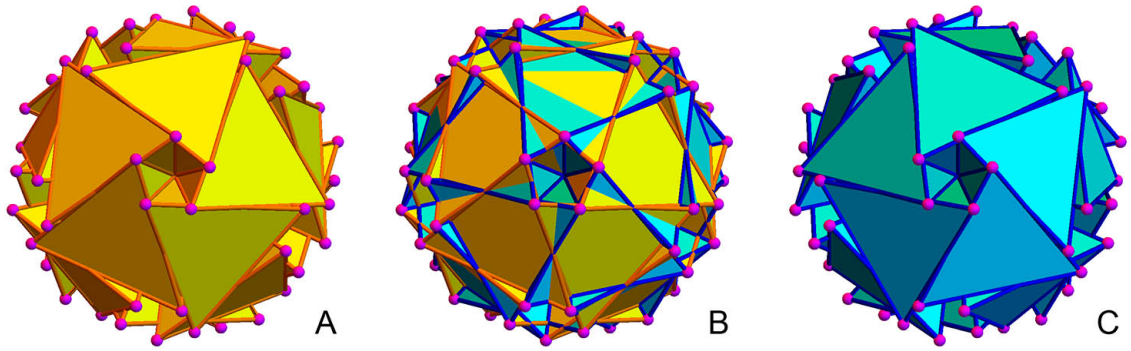

Figure 9: *A) The right twisted 20G, B) The superposition of the left-twisted and right-twisted 20G.*

Elser-Sloane quasicrystal

The Elser-Sloane quasicrystal is a four-dimensional quasicrystal obtained via cut-and-project or Hopf mapping from the eight-dimensional lattice E_8[7,6]. The mapping matrix of the cut-and-project method is given below[6]

$$\Pi = -\frac{1}{\sqrt{5}}\begin{bmatrix} \tau I & H \\ H & \sigma I \end{bmatrix},$$

where $I = I_4 = diag\{1,1,1,1\}$, $\sigma = \frac{\sqrt{5}-1}{2}$ and

$$H = \frac{1}{2}\begin{bmatrix} -1 & -1 & -1 & -1 \\ 1 & -1 & -1 & 1 \\ 1 & 1 & -1 & -1 \\ 1 & -1 & 1 & -1 \end{bmatrix}.$$

The point group of the resulting quasicrystal is $H_4 = [3,3,5]$, the largest finite real four-dimensional group[2]. It is the symmetry group of the regular four-dimensional polytope, the 600-cell. H_4 can be shown to be isomorphic to the point group of E_8 using quaternions[5] and it is inherently both four-dimensional and eight-dimensional.

The unit icosians, a specific set of Hamiltonian quaternions with the same symmetry as the 600-cell, form the 120 vertices of the 600-cell with unit edge length. They can be expressed in the following form:

$(\pm 1, 0, 0, 0)$, $\frac{1}{2}(\pm 1, \pm 1, \pm 1, \pm 1)$, $\frac{1}{2}(0, \pm 1, \pm 1, \pm\sigma, \pm\tau)$ with all even permutations of the coordinates. The quarternionic norm of an icosian $q = (a,b,c,d)$ is $a^2+b^2+c^2+d^2$, which is a real number of the form $A + B\sqrt{5}$, where $A, B \in \mathbb{Q}$. The Euclidean norm of q is $A + B$ and it is greater than zero. With respect to the quarternionic norm, the icosians live in a four-dimensional space. It can be shown that the Elser-Sloan quasicrystal is in the icosian ring, finite sums of the 120 unit icosians. Under the Euclidean norm, the icosian ring is isomorphic to an E_8 lattice in eight dimension. There are 240 icosians of Euclidean norm 1 with 120 being the unit icosians and the other 120 being σ times the unit icosians. How these icosians corresponds to the 240 minimal vectors, $e_n, n = 1,2,...,8$ of the E_8 lattice is shown in Table 1.

One type of three-dimensional cross-sections of the Elser-Sloane quasicrystal forms quasicrystals with icosa-

Table 1: *Correspondence between the icosians and the E_8 root vectors*

Icosians	E_8 root vectors
$(1,0,0,0)$	e_1+e_5
$(0,1,0,0)$	e_1+e_5
$(0,0,1,0)$	e_1+e_5
$(0,0,0,1)$	e_1+e_5
$(0,\sigma,0,0,)$	$\frac{1}{2}(-e_1-e_2+e_3+e_4+e_5+e_6-e_7-e_8)$
$(0,0,\sigma,0)$	$\frac{1}{2}(-e_1-e_2-e_3+e_4+e_5+e_6+e_7-e_8)$
$(0,0,0,\sigma)$	$\frac{1}{2}(-e_1-e_2-e_3-e_4+e_5+e_6+e_7+e_8)$

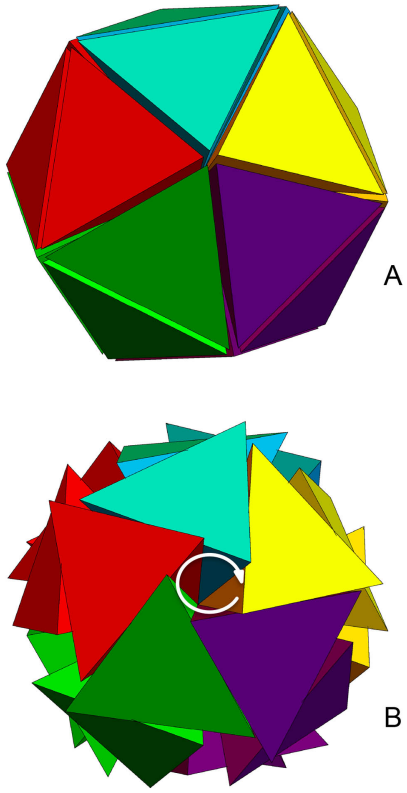

Figure 10: *A) An evenly distributed vertex-sharing-20-tetrahedra cluster and B) a twisted 20G with maximum plane class reduction.*

hedral symmetry and the other type forms quasicrystals with tetrahedral symmetry. The Fibonacci icosagrid is related to both types of quasicrystals. The icosahedral cross-section of the Elser-Slaone quasicrystal has the same types of unit cells (Fig. 14B) and is of the same symmetry group as the space-filling analog of the Fibonacci icosagrid (Fig. 14A) introduced in the earlier section. The five-compound of the tetrahedral quasicrystals turned out to be a subset of the Fibonacci icosagrid. Details are discussed in the following sections.

Compound quasicrystals

The center of the Esler-Slaone quasicrystal is a unit-length 600-cell. Since it is closed under τ scaling, there is an infinite number of concentric 600-cells that are sizes of powers of the golden ratio. There is also an infinite number of unit-length 600-cells at different locations in the quasicrystal but none of them intersect each other. For the golden-ratio-length 600-cells, they touch or intersect with each other in 8 different ways (Fig. 15). Each 600-cell has 600 regular tetrahedral facets. The Elser-Sloane quasicrystal has two kinds of three-dimensional tetrahedral cross-sections in relation to the center 600-cell. The first, type I, (shown in Fig. 16A) is a cross-section through the equator of the center 600-cell. It has four vertex sharing tetrahedra at its center with their edge length τ times the edge length of the 600-cell. The second, type II, (shown in Fig. 17A) is a cross-section through a facet of the 600-cell. As a result, it has smaller unit-length tetrahedral cells, with only one at the center of the cross-section. Both cross-sections are quasicrystals. As we can see from Fig. 16A and Fig. 17A, the type I cross-section is a much denser packing of regular tetrahedra compared with type II. They both appear as a subset of the Fibonacci tetragrid. More rigorous proof will be included in future papers but here we will present a brief proof in the following paragraph.

The substitution rules for the Fibonacci sequence are $L \to LS$ and $S \to L$. In other words, both segments are inflated by the golden ratio τ scaling. Therefore the Fibonacci chain is closed by τ scaling and we can call it a τ chain. As we mentioned earlier, the Elser-Sloane quasicrystal is also closed by τ. A cross-section, as a subset of the quasicrystal will have one-dimensional chains that are subsets of the τ chain. Then it is not hard to prove that these tetrahedral cross-sections are a subset of the Fibonacci tetragrid.

Using the same golden composition method as used in the construction of the Fibonacci icosagrid with the Fibonacci tetragrid, a compound quasicrystal of type I (Fig. 16B) can be generated with five copies of type I cross-sections. And similarly, a type II compound quasicrystal (Fig. 16B) can be generated with 20 copies of slices at type II tetrahedral cross-sections. Both compound quasicrystals recovered their lost five-fold symmetry from the tetrahedral cross-section and became icosahedrally symmetric.

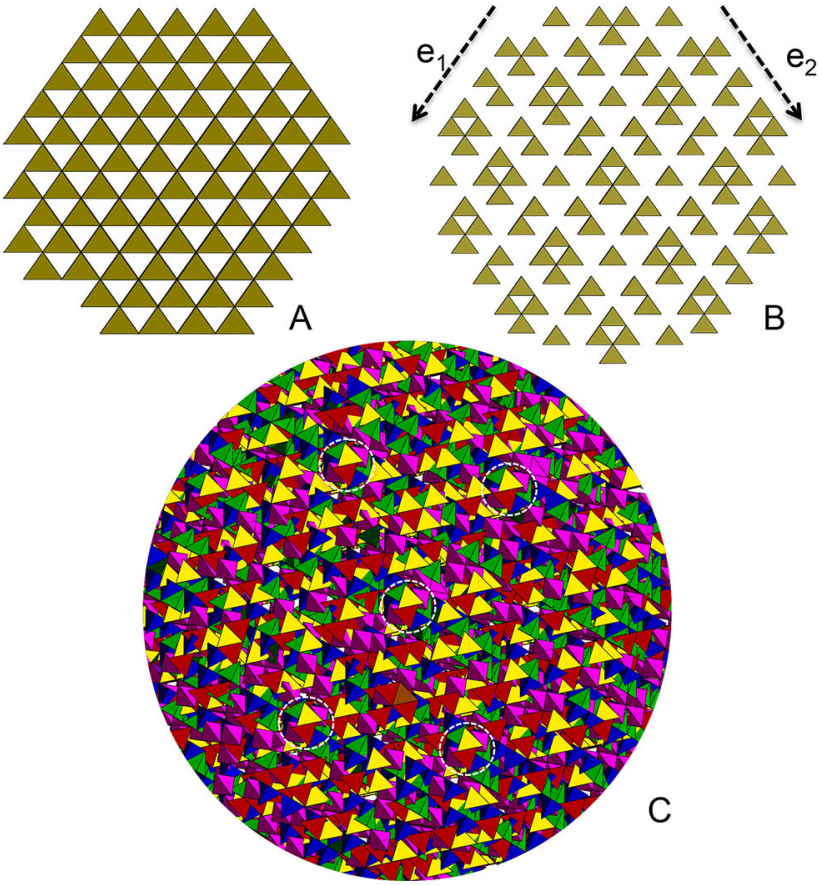

Figure 11: *A) A 2D projection of a tetragrid, B) a 2D projection of a Fibonacci tetragrid, C) a sample Fibonacci IcosaGrid. Notice that 20Gs formed up at the locations marked with while dotted circles.*

V. Connections between the Fibonacci icosagrid and E_8

It is clear from the above discussion that both compound quasicrystals are subsets of the Fibonacci icosagrid. More over, the type II compound quasicrystal is a subset of the type I compound quasicrystal 18. Indeed, the Fibonacci icosagrid can be obtained from the cross-sections of the Elser-Sloane quasicrystal with a process called "enrichment" - defined as a procedure to add necessary planar grids to make the cross-sections a complete Fibonacci tetragrid. After this "enrichment" process, the compound quasicrystal becomes the Fibonacci icosagrid. This establishes the connection between the Fibonacci icosagrid, the Elser-Sloane quasicrystal and E_8. In fact, we intend to model the fundamental particles and forces with the Fibonacci icosagrid, which is a network of Fibonacci chains. Henceforth, we name the Fibonacci icosagrid the quasicrystalline spin-network.

Finally we want to point out the importance of the golden composition procedure for composing the compound quasicrystal. It not only significantly reduces the plane classes, compared to the evenly distributed 20-tetrahedra cluster, but also makes the composition a quasicrystal. In other words, the reason we use the golden composition process to compose the cross sections together to form the compound quasicrystal is the same for introducing the Fibonacci spacing in the icosagrid, to convert the structure into a perfect quasicrystal. Fig. 20 shows the steps of this convergence. An interesting fact is that the dihedral angle of the 600-cell is the golden angle plus 60 degrees. Notice that the process, golden composition, which is manually introduced here to make the compound quasicrystal a perfect quasicrystal, comes up naturally in the quasicrystalline spin-network when derived from the icosagrid. While the other process, Fibonacci spacing, which is manually introduced to the icosagrid to convert it to a quasicrystal, emerges naturally in the Elser-Sloane quasicrystal, therefore the three-dimensional cross-sections of the Esler-Sloane quasicrystal.

VI. Conclusions

This paper has introduced a method, the Fibonacci multigrid method, to convert the grid space into a quasicrystal. Using this method, we generated an icosahedral quasicrystal the quasicrystalline spin-network. We have shown a mapping between the Fibonacci icosagrid and the quasicrystals derived from E_8. The compound quasicrystals derived from the Elser-Sloane quasicrystal thus from E_8 too, are subsets of the Fibonacci icosagrid and they can be "enriched" to become the Fibonacci

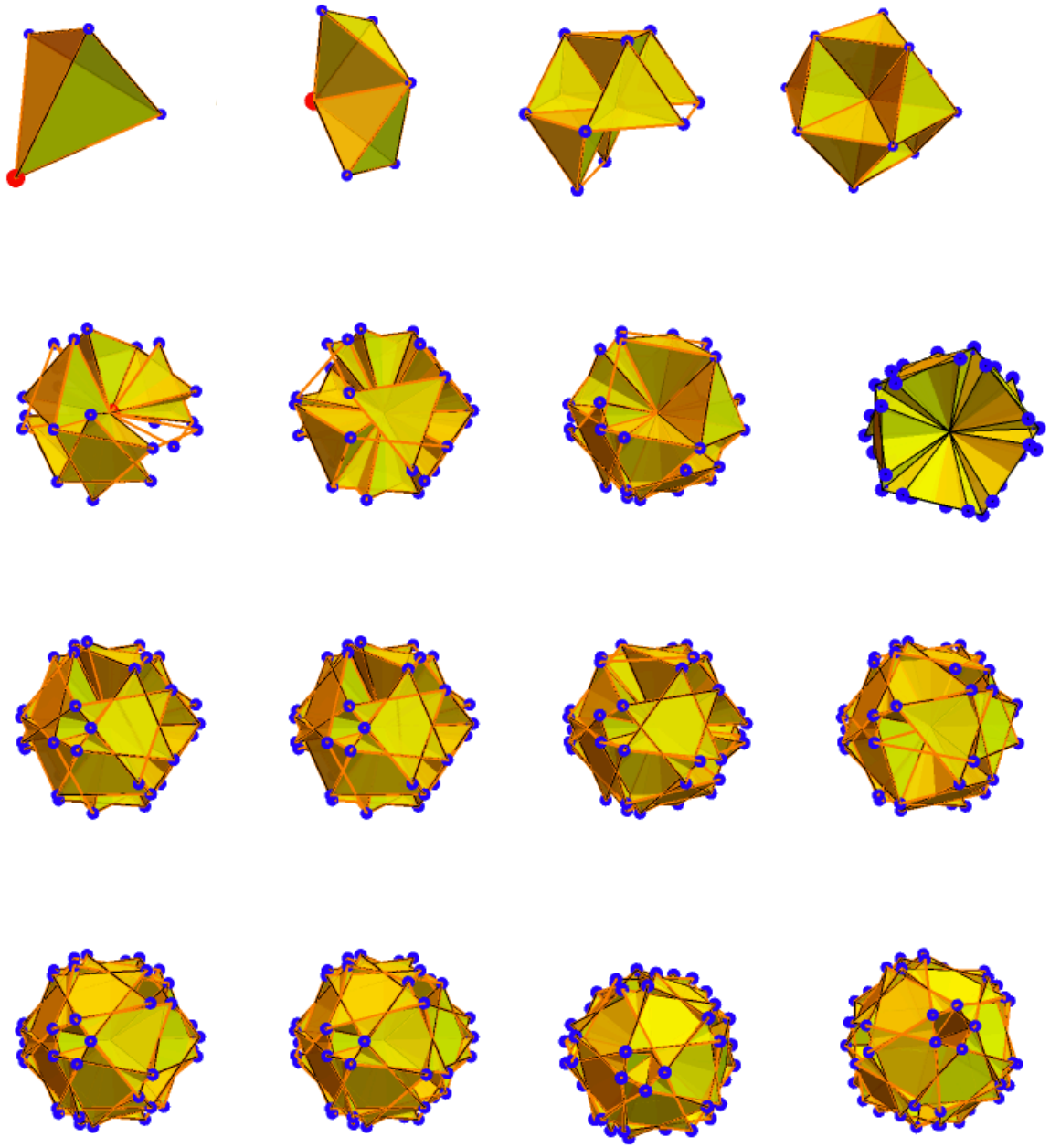

Figure 12: *A sample list of vertex configuration in the Fibonacci icosagrid.*

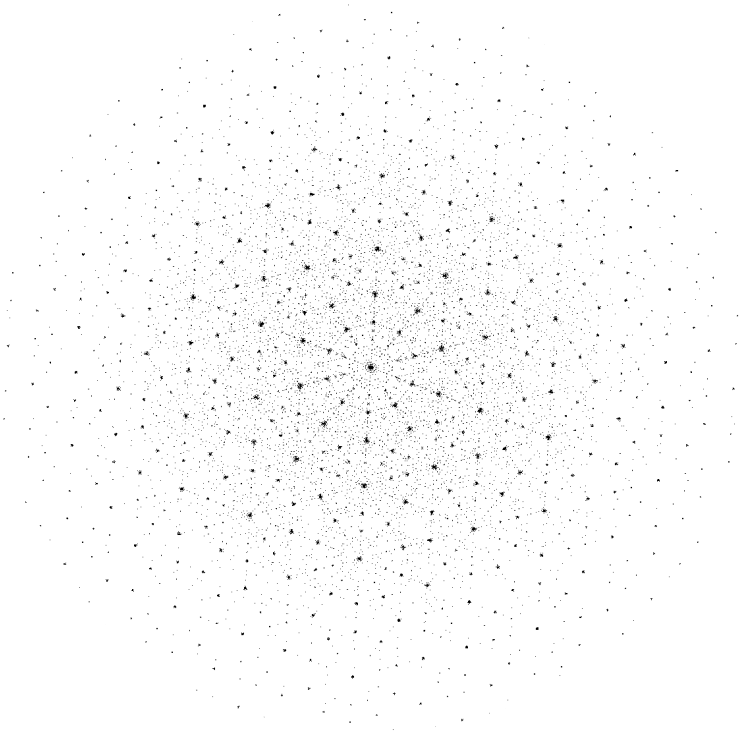

Figure 13: *Diffraction pattern down the five-fold axis of the point space obtained by taking the vertices of the tetrahedra.*

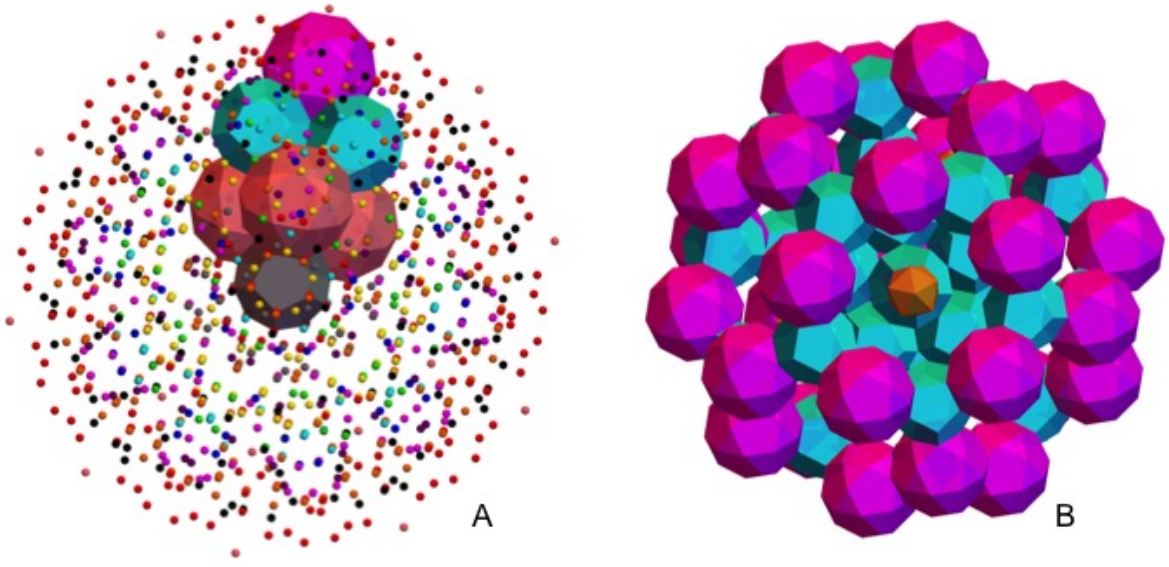

Figure 14: *A) Space-filling analog of the Fibonacci icosagrid, B) An icosahedral cross-section of the Elser-Sloane quasicrystal.*

icosagrid. We conjecture that exploring such an aperiodic point space based on higher dimensional crystals may have applications for quantum gravity theory.

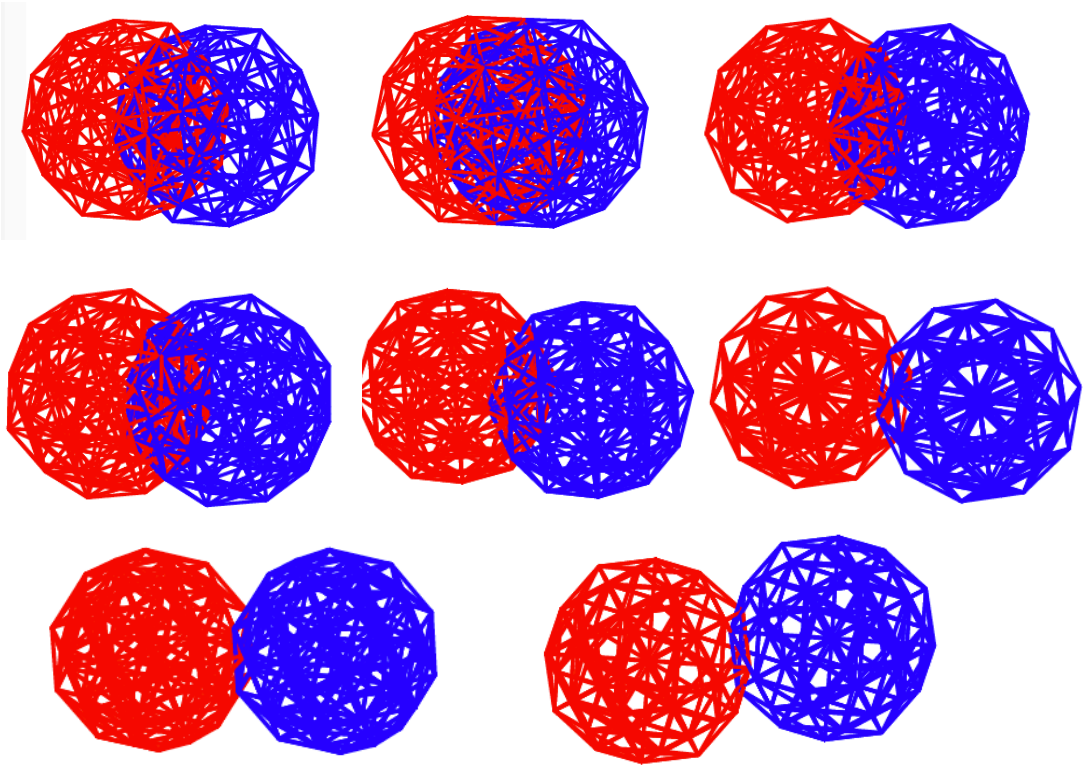

Figure 15: *Two-dimensional projection of the 8 types of golden-ratio-length 600-cell intersections.*

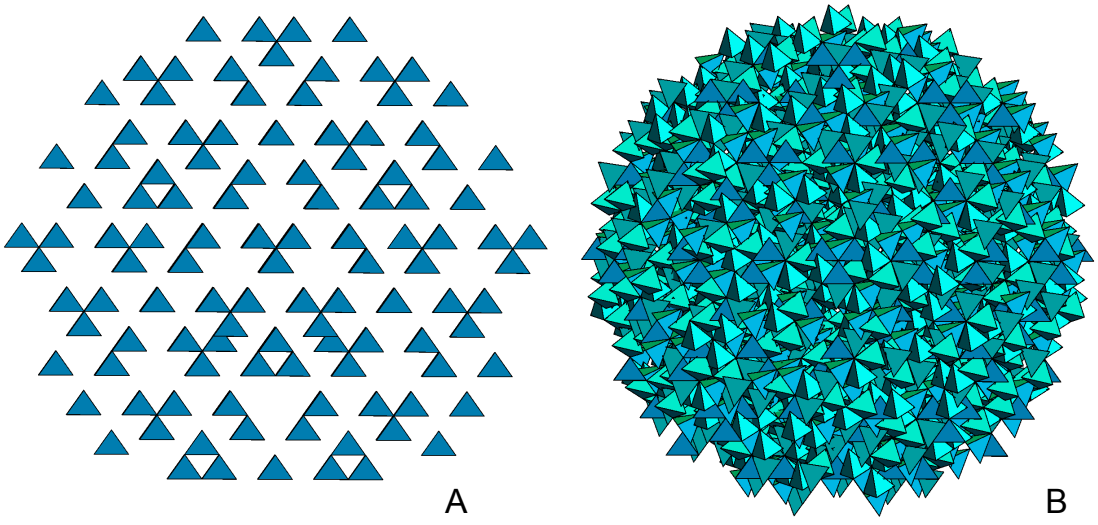

Figure 16: *A) Type I tetrahedral cross-section of the Elser-Sloane quasicrystal, B) The compound quasicrystal*

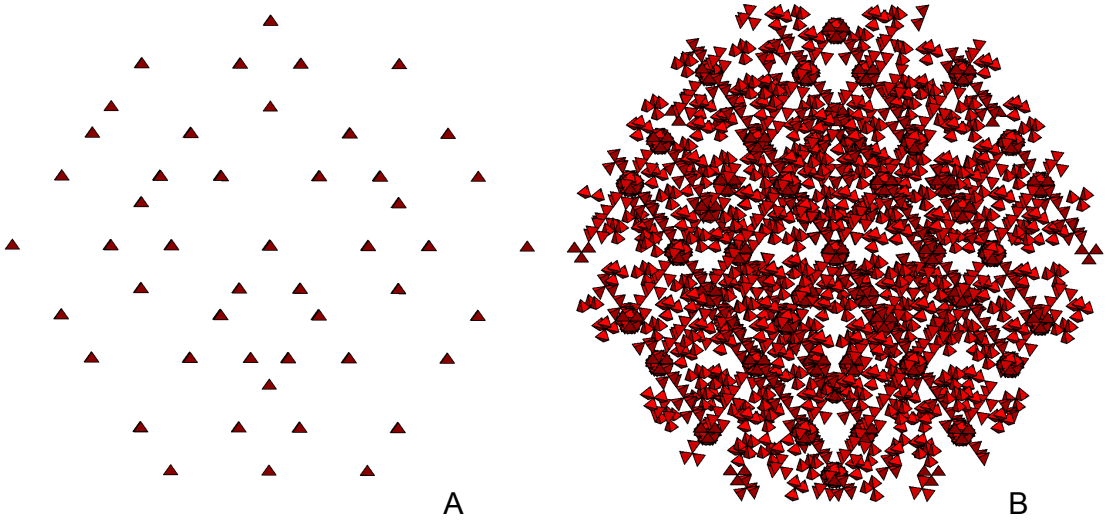

Figure 17: *A) Type II tetrahedral cross-section with τ scaled tetrahedra, B) The more sparse CQC*

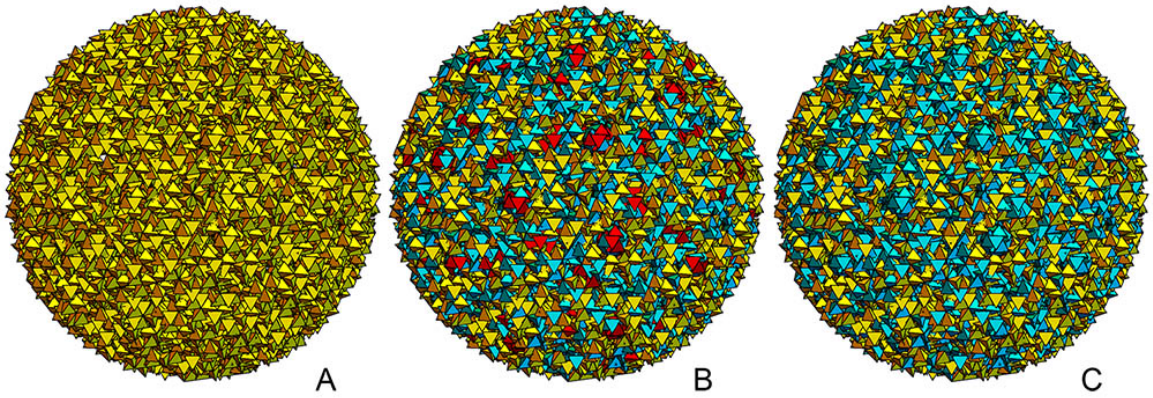

Figure 18: *A) Tetrahedra of the Fibonacci icosagrid, B) Cyan highlighted tetrahedra belong to the Type II compound, C) Red highlighted tetrahedra belong to the Type I compound*

Corresponding Author •fang@quantumgravityresearch.org

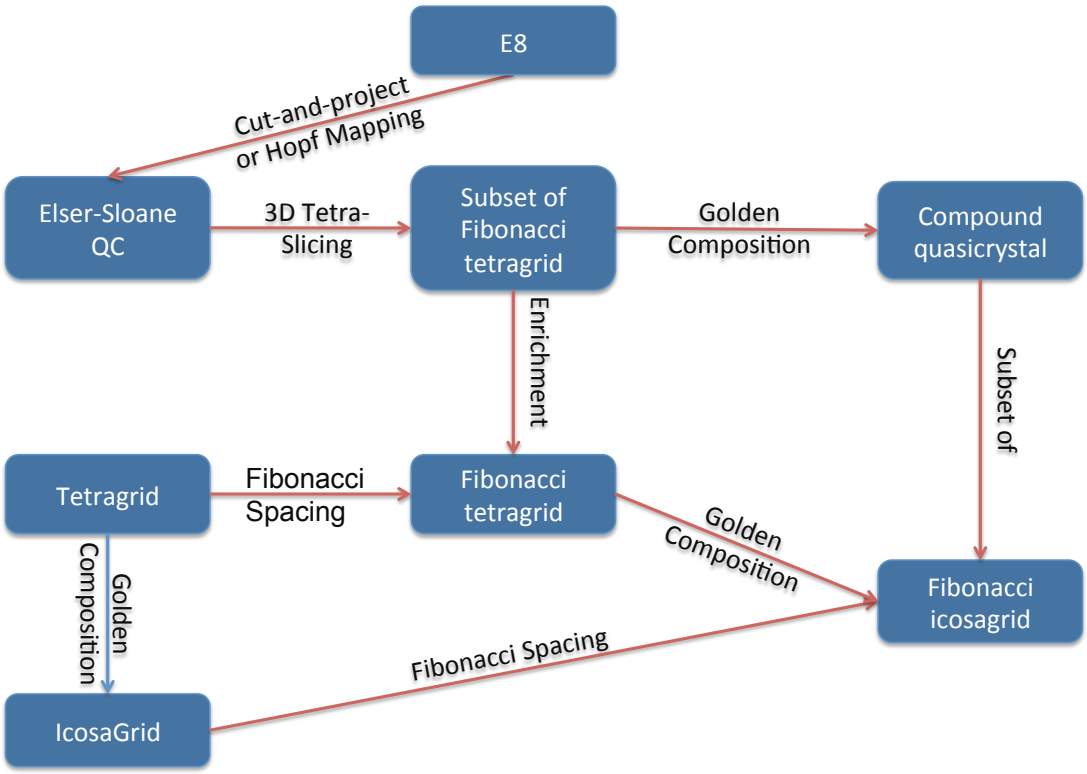

Figure 19: *The relationships between FIG and CQC and how they are generated.*

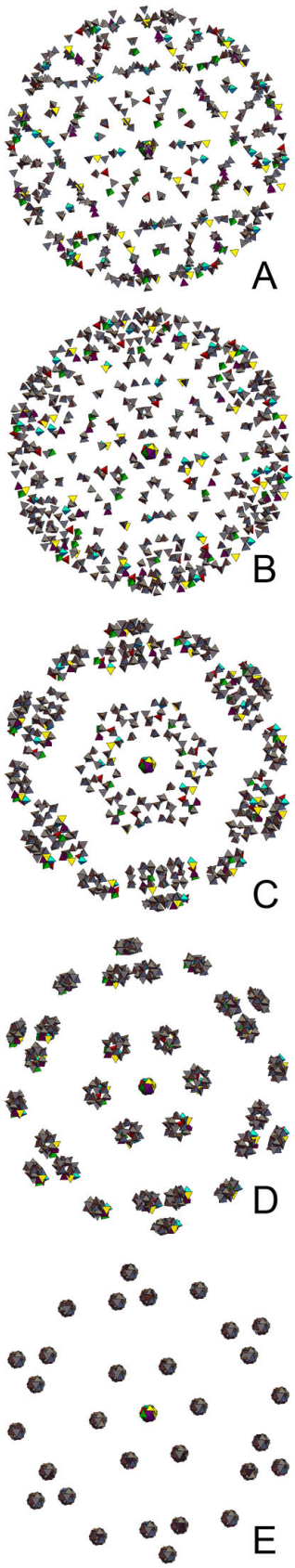

Figure 20: *Convergence of the outer 20Gs, from A to E as the angle of rotation in the golden composition slowly increased from 0 to the golden angle.*

References

[1] M. Baake and U. Grimm. *Aperiodic Order*. Cambrage University Press, 2013.

[2] H. F. Blichfeldt. *Finite Collineation Groups*. University of Chicago Press, 1917.

[3] N. D. Bruijn. Algebraic theory of penrose's non-periodic tilings of the plane. *Indagationes Mathematicae (Proceedings)*, 84(1):39–66, 1981.

[4] A. Connes. *Non-Commutative Geometry*. Springer, 1988.

[5] J. Conway and N. Sloane. *Sohere Packing, Lattices and groups*. Springer, 1998.

[6] V. Elser and N. J. A. Sloane. A highly symmetric four-dimensional quasicrystal. *J. Phys. A*, 20:6161–6168, 1987.

[7] B. et al. Photonic band gap phenomenon and optical properties of artificial opals. *Physical Review E*, 55(6):7619, 1997.

[8] F. Fang, K. Irwin, J. Kovacs, and G. Sadler. Cabinet of curiosities: the interesting geometry of the angle = arccos((3 - 1)/4) cabinet of curiosities: the interesting geometry of the angle = arccos((3 - 1)/4). *ArXiv:1304.1771*, 2013.

[9] I. Fisher, Z. Islam, A. Panchula, K. Cheon, M. Kramer, P. Canfield, and A. Goldman. Growth of large-grain r-mg-zn quasicrystals from the ternary melt (r= y, er, ho, dy and tb). *Philosophical Magazine B*, 77(6):1601–1615, 1998.

[10] C. L. Henley. Cell geometry for cluster-based quasicrystal models. *Physical Review B*, 43(1):993, 1991.

[11] D. Levine and P. J. Steinhardt. Quasicrystals: a new class of ordered structures. *Physical review letters*, 53(26):2477, 1984.

[12] D. Levine and P. J. Steinhardt. Quasicrystals. i. definition and structure. *Physical Review B*, 34(2):596, 1986.

[13] R. Lifshitz. The definition of quasicrystals. *arXiv:cond-mat/0008152 [cond-mat.mtrl-sci]*, 2000.

[14] J. Miekisz and C. Radin. The unstable chemical structure of quasicrystalline alloys. *Physics Letters A*, 119(3):133–134, 1986.

[15] R. Moody, editor. *The Mathematics of Long-Range Aperiodic Order*, volume 489. Springer Netherlands, 1997.

[16] R. V. Moody and J. Patera. Quasicrystals and icosians. *Journal of Physics A: Mathematical and General*, 26(12):2829, 1993.

[17] J. Patera, editor. *Quasicrystals and discrete geometry*, volume 10. American Mathematical Soc., 1998.

[18] S. Poon. Electronic properties of quasicrystals an experimental review. *Advances in Physics*, 41(4):303–363, 1992.

[19] N. Rivier. A botanical quasicrystal. *Le Journal de Physique Colloques*, 47(C3):C3–299, 1986.

[20] J. Sadoc and R. Mosseri. The e8 lattice and quasicrystals. *Journal of non-crystalline solids*, 153:247–252, 1993.

[21] M. L. Senechal. *Quasicrystals and Geometry*. Cambrige University Press, 1995.

[22] D. Shechtman, I. Blech, D. Gratias, and J. W. Cahn. Metallic phase with long-range orientational order and no translational symmetry. *Physical Review Letters*, 53(20):1951, 1984.

[23] J. E. Socolar, T. Lubensky, and P. J. Steinhardt. Phonons, phasons, and dislocations in quasicrystals. *Physical Review B*, 34(5):3345, 1986.

[24] J. E. Socolar and P. J. Steinhardt. Quasicrystals. ii. unit-cell configurations. *Physical Review B*, 34(2):617, 1986.

[25] P. J. Steinhardt and S. Östlund. *Physics of quasicrystals*. World Scientific, 1987.

[26] W. Steurer and S. Deloudi. *Crystallography of Quasicrystals: Concepts, Methods and Structures*. Springer Science and Business Media, 2009.

[27] A. Tsai, J. Guo, E. Abe, H. Takakura, and T. Sato. Alloys: A stable binary quasicrystal. *Nature*, 408(6812):537–538, 2000.

Corresponding Author •fang@quantumgravityresearch.org